

Titre: Copper precipitation at engine operating temperatures in powder-forged connecting rods manufactured with Fe-Cu-C alloys

Auteurs: Edmond Ilia, Philippe Plamondon, Jean-Philippe Masse, & Gilles L'Espérance

Date: 2019

Type: Article de revue / Article

Référence: Ilia, E., Plamondon, P., Masse, J.-P., & L'Espérance, G. (2019). Copper precipitation at engine operating temperatures in powder-forged connecting rods manufactured with Fe-Cu-C alloys. *Materials Science & Engineering A*, 767, 138383 (9 pages). <https://doi.org/10.1016/j.msea.2019.138383>

Document en libre accès dans PolyPublie

Open Access document in PolyPublie

URL de PolyPublie: <https://publications.polymtl.ca/4944/>

PolyPublie URL:

Version: Version officielle de l'éditeur / Published version
Révisé par les pairs / Refereed

Conditions d'utilisation: Creative Commons Attribution-Utilisation non commerciale-Pas d'oeuvre dérivée 4.0 International / Creative Commons Attribution-NonCommercial-NoDerivatives 4.0 International (CC BY-NC-ND)

Terms of Use:

Document publié chez l'éditeur officiel

Document issued by the official publisher

Titre de la revue: *Materials Science & Engineering A* (vol. 767)

Journal Title:

Maison d'édition: Elsevier B.V.

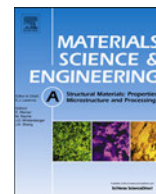
Publisher:

URL officiel: <https://doi.org/10.1016/j.msea.2019.138383>

Official URL:

Mention légale:

Legal notice:



Copper precipitation at engine operating temperatures in powder-forged connecting rods manufactured with Fe–Cu–C alloys

Edmond Ilia^a, Philippe Plamondon^b, Jean-Philippe Masse^b, Gilles L'Espérance^{b,*}

^a American Axle and Manufacturing, Detroit, MI, 48211-1198, USA

^b École Polytechnique de Montréal, Center for Characterization and Microscopy of Materials, (CM)², Montréal, Québec, Canada

ARTICLE INFO

Keywords:

Cu precipitation
Fe–Cu–C alloys
Powder Forging
Connecting Rods
Mechanical Properties

ABSTRACT

The effect of copper precipitation on the mechanical properties of Fe–Cu–C alloys prepared for Powder Metallurgy and used to manufacture connecting rods for the automotive industry through powder forging was evaluated at engine operating temperatures, ranging between 100 °C and 150 °C. Tensile tests were conducted at room temperature as well as at 120 °C and 150 °C on specimens machined from connecting rods. The test results clearly indicated an improvement in the strength of Fe–Cu–C alloys at 120 °C and 150 °C. Scanning and transmission electron microscopies were employed to investigate the strengthening mechanism causing the improvement. The microscopy investigations pointed to stress-induced second phase precipitation strengthening in super-saturated Fe–Cu–C alloys even at these relatively low temperature levels as copious Cu nano precipitates were observed in the specimens submitted to tensile testing at 120 °C and components submitted to engine dynamometer testing. Clear evidence of interactions between dislocations and copper precipitates was found in both tensile specimens and components.

1. Introduction

Several methods such as cold working, solid solution strengthening, grain refining, and second phase precipitation hardening are widely employed to improve the strength of alloys used to manufacture structural components. In particular, in the case of Fe–Cu–C alloys prepared for Powder Metallurgy (PM) and employed to manufacture almost 100% of the powder-forged (PF) connecting rods for the automotive industry globally, copper and graphite powders are uniformly admixed in a pure iron powder, produced through water atomization and annealed to improve the compressibility, as well as reduce oxygen and carbon levels (< 0.01% C). Both of these additives efficiently and cost-effectively improve the strength and hardness of steel through solution strengthening. However, it is important to note that, because of the mixing process during the manufacturing of powder-based Fe–Cu–C alloys, some level of chemical composition inhomogeneity is expected.

In particular, copper, known for its instrumental role during sintering, is effective in inhibiting the growth of new grains formed during recrystallization that takes place after hot forging [1]. Furthermore, copper additions shift the eutectoid composition towards pure iron, thus increasing the amount of pearlite in the microstructure and, ultimately the strength. Lastly, copper, which has a relatively high solubility in iron at high temperatures, but displays continuously decreasing

solubility at lower temperatures, can provide additional strengthening through precipitation during a subsequent aging treatment.

There is a limited amount of information available in the literature on the effect of aging and copper precipitation strengthening mechanisms of powder-forged Fe–Cu–C alloys. In one recent paper, Wang et al. studied the effect of the Cu content on the microstructure and mechanical properties of powder-forged connecting rods manufactured with Fe–Cu–C alloys. Cu precipitates with a diameter of about 10 nm were observed in the microstructure of the forged parts. Although the volume fraction of these precipitates increased with the Cu content, the authors concluded that grain refinement was the main strengthening mechanism associated with Cu addition. They suggested that Cu precipitates, consisting of a soft material, would be easily sheared by the dislocations [2].

However, in another paper, Nakashima et al. carried out TEM observations on wrought Fe–Cu steels and observed multiple nanoscale Cu precipitates tangled in dislocations. Orowan loops were not observed around the smallest Cu precipitates which suggests they were not cut by the dislocations. The authors concluded that the Cu precipitates must be smaller than a critical size of about 70 nm to result in precipitation strengthening of Fe–Cu alloys [3].

In addition, there are several studies focusing on aging and copper precipitation of as-sintered Fe–Cu–C PM alloys. Kapoor studied the

* Corresponding author.

E-mail addresses: edmond.ilia@aam.com (E. Ilia), gilles.lesperance@polymtl.ca (G. L'Espérance).

effect of copper content, cooling rate after sintering, as well as aging at different temperatures for different times on the strength of sintered Fe–Cu PM alloys. He concluded that “under proper heat treating conditions, it is possible to increase the strength of 2% copper [Fe–Cu PM alloys] compacts by almost 60% and for 4% copper compacts [Fe–Cu PM alloys] by 50%.” In addition, it was shown that peak strength was achieved after aging at 500 °C for 2 h [4].

In another work on Fe powder-based materials alloyed with copper (compacted and sintered), it was shown that the presence of Cu precipitates in material contributes to increasing the hardness. By using nano-indentations and scanning electron microscopy (SEM), areas containing nanometric Cu precipitates led to a hardness increase of up to 23% in the case of alloys aged at 500 °C. However, a decrease in hardness was observed in the case of the other aging temperatures considered (300 °C and 700 °C) [5].

Although the mechanical properties of the materials used to manufacture connecting rods have been widely characterized at room temperature (RT) [6,7], their strength has not been investigated at engine operating temperatures, until recently [8,9]. It has been reported that a typical temperature in the piston pin boss is approximately 200 °C [10]. In the case of a diesel engine, a temperature of 125 °C was measured in the small end of a connecting rod, which represents the most stressed area of the component in operation [11]. Typically, the operating temperature of connecting rods in the minimum cross-section of the I-beam can range between 100 °C and 150 °C, depending on engine type and characteristics.

Extensive studies on the effect of higher temperatures on the mechanical properties of construction steels have produced empirical formulae to evaluate the strength at any given temperature if the strength at room temperature is known [12,13]. Employing a formula developed by Ancas et al. [12], a reduction in proportional strength of approximately 4% is expected at 100 °C, followed by reductions of approximately 5% and 7% at 120 °C and 150 °C, respectively.

Ilia investigated the mechanical properties of powder-forged Fe–Cu–C alloys containing 3% Cu and 3.25% Cu at 120 °C and 150 °C. Despite the results obtained by Ancas et al. it was shown that mechanical properties of powder-forged Fe–Cu–C alloys are higher at 120 °C than at room temperature. SEM and transmission electron microscopy (TEM) investigations revealed the presence of copious nano precipitates of copper in the specimens submitted to tensile testing at 120 °C [8].

This work was undertaken to investigate the strengthening mechanism causing the improvement of mechanical properties as a result of copper precipitation even at the relatively low temperature of 120 °C and the interaction between the precipitates and dislocations during deformation.

2. Materials and methods

2.1. Sample preparation

Manufacturing of powder-forged connecting rods entails powder pressing into a compact approximately 15% porous that is sintered at high temperature levels in a furnace in a protective atmosphere consisting of nitrogen and hydrogen. Subsequently, the sintered compact is hot forged (re-pressed) to almost fully dense conditions and cooled in still air. A typical density of powder-forged connecting rods ($\sim 7.84 \text{ g/cm}^3$) is higher than 99.5% of the theoretical density of the material.

Over the years, the chemical composition of Fe–Cu–C alloys employed to fabricate powder-forged connecting rods has been optimized to achieve maximum performance. Mechanical properties of Fe–Cu–C alloys with different copper content (ranging from 2% to 4%, in incremental steps of 0.5%) and carbon content (ranging from 0.50% to 0.70%, in incremental steps of 0.07%) in powder-forged conditions were evaluated. Tensile testing on cylindrical specimens machined from the I-beam area of connecting rods, Fig. 1, clearly showed that by

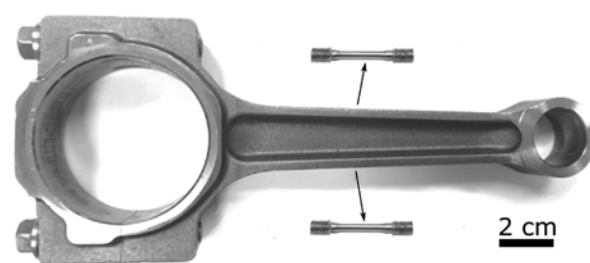


Fig. 1. Tensile specimens and the location from where they were obtained in the component.

increasing copper additions from 2.0% to 3.0%, an improvement of 140 MPa (16%) was obtained in ultimate tensile strength (UTS) in the material with 0.50% carbon. For the same 1% increase in copper addition, the yield strength (YS) improved by 150 MPa (27%). YS reached the maximum value at 3.25% Cu; however, the most important conclusion from these results is represented by the fact that both UTS and YS are very stable in the copper range from 3.0% to 3.50%, thus resulting in not only higher but more consistent mechanical properties within this interval. In addition, it was noted that copper had a larger effect in improving YS than it had in improving UTS [6].

On the other hand, significant improvements in UTS and YS were observed when the carbon content was increased up to 0.64%. Only modest improvements were obtained afterwards by further increasing the carbon content to 0.70%. It was found that higher carbon contents had a larger effect in improving UTS (approximately 13%) than YS (approximately 9%). Thus, carbon and copper complement each other well as cost-effective strengtheners of PF Fe–Cu–C alloys [6].

The nominal chemical composition of most of the materials used to manufacture powder-forged connecting rods is summarized in Table 1 while their mechanical properties at RT are summarized in Table 2. In the case of the material designations used in the tables, the letter L stands for low, the letter M stands for mid, and the letter H stands for high. In addition, the letter S stands for strength, while the three digits represent the approximate ultimate tensile strength of the material in 10^3 psi , rounded to the nearest tenth. In the case of HS170 M, the most widely used material in mass production by the powder-forging industry to manufacture connecting rods for automotive applications, the letter M at the end stands for modified [6]. This material represents the optimized chemical composition of the Fe–Cu–C alloys for maximum strength for powder-forged connecting rods under mass-production conditions. The typical microstructure of these materials is pearlitic-ferritic, with pearlite content ranging from $\sim 75\%$ in the case of LS120 and up to $\sim 90\%$ in the case of HS170 M.

2.2. Strength test results

Cylindrical specimens (Fig. 1) machined from the I-beam area of connecting rods manufactured through powder forging under mass production conditions were submitted to tensile testing. Tensile tests at RT, in accordance with ASTM Standard E8/8M-16A [14], as well as at

Table 1

Typical chemical composition of connecting rod materials.

	Cu ^a	C ^b	MnS ^a	Fe
LS120 (ASTM PF-11C50)	2.00	0.475	0.32	Bal.
MS130 (ASTM PF-11C60)	2.00	0.575	0.34	Bal.
HS150 (ASTM PF-1130C50)	3.00	0.475	0.32	Bal.
HS160 (ASTM PF-1130C60)	3.00	0.575	0.34	Bal.
HS170 M (ASTM PF-1135C60)	3.25	0.640	0.32	Bal.

^a Added to the mix.

^b Measured in the as-forged product.

Table 2
Mechanical properties at room temperature.

RT	LS120	MS130	HS150	HS160	HS170 M
UTS (MPa)	884.3	961.8	1030.4	1079.2	1200.7
YS (MPa)	592.1	604.2	728.5	738	854.1
Elongation (%)	18	14.6	14.5	13	11.6
Area Reduction (%)	24.9	23.2	22.7	18.7	17.8

120 °C and 150 °C, in accordance with ASTM Standard E21-09 [14], were conducted at Westmoreland Mechanical Testing and Research Inc., Youngstown, PA, using a Thermcraft furnace chamber (soaking time 30 min). A minimum of fifteen specimens were submitted to tensile testing at each temperature. A typical stress-strain curve obtained from tensile testing of HS170 M at 120 °C as well as typical fracture surfaces obtained after testing at RT, 120 °C, and 150 °C are shown in Fig. 2. The shape of all the stress-strain curves was similar except for the values of the YS, UTS, and elongation. No differences in morphology were observed on the fracture surfaces.

The tensile test results at engine operating temperature levels clearly showed that the strength of HS170 M improves at 120 °C and slightly decreases afterwards at 150 °C, still remaining above the strength at room temperature (Fig. 3). Thus, the UTS at 120 °C improved by 5.5%, while the YS at the same temperature improved by 5.2%. In addition, when the testing temperature is increased to 150 °C, this improvement in strength is maintained, although to a lesser extent, as the UTS at 150 °C is higher by 3.1% than the value at room temperature, while the YS at the same temperature is still higher by 0.3% over the value at room temperature [8].

Similar results were obtained from the other Fe–Cu–C based materials, as illustrated in Fig. 4. As shown, Fe–Cu–C alloys exhibit a very similar behavior: the tensile strength improves at 120 °C and slightly drops at 150 °C, typically remaining above the strength at room temperature [8].

2.3. Microstructural characterization techniques

Sections cut from connecting rods submitted to engine dynamometer testing (dyno testing) and tensile specimens tested at RT and 120 °C, as shown in Fig. 5, were submitted to electron microscopy investigations.

A high-resolution field emission gun scanning electron microscope (JEOL JSM-7600F) equipped with a low angle backscattered electron detector (LABE) and an X ray EDS detector was used. A detailed investigation with a field emission gun transmission electron microscope (JEOL JEM-2100F) equipped with EDS and STEM detectors was also performed.

For the SEM observations, the final polishing of the specimen surface is very important. To image the nanometric Cu precipitates, a Buehler Chemomet™ cloth with a 50 nm alumina colloidal suspension was used for the final polishing. SEM observations were also employed to determine the best locations to prepare TEM thin lamellae by focused ion beam (FIB).

The FIB used in this study is a JEOL 4700F equipped with a Ga⁺ source operated at 30 kV for the initial polishing. Final polishing was done in the JEOL Ion Slicer using argon gas at 3 kV. One of the main advantages of the FIB, which was very useful for this work, is that it allows preparing a thin lamella for TEM from an area of interest previously selected under the optical microscope or SEM.

A Clemex™ microhardness tester was used for hardness measurements. The specimens were prepared in the same way as for the SEM observations. The image analysis was conducted with the Clemex Vision PE™ software. Since the material comprises areas without Cu, therefore without Cu precipitates, the proportion of fields containing Cu precipitates was calculated in order to correct the volume fraction of precipitates measured in areas containing Cu precipitates. A large number of images, between forty and sixty, was acquired at random locations and those containing Cu precipitates were analyzed by image analysis. Because of the weak contrast between the matrix and the precipitates, which are smaller than 30 nm, it was not possible to automatically discriminate them from the matrix using a greyscale

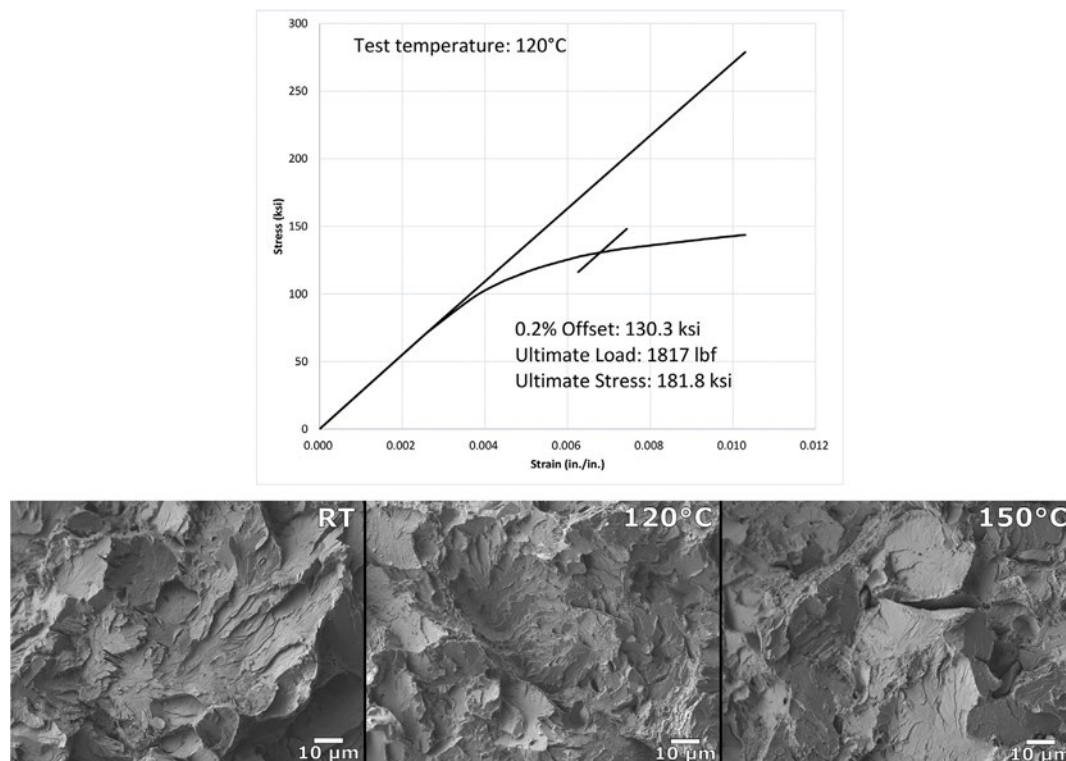


Fig. 2. Stress-strain curve obtained from tensile testing at 120 °C and fracture surfaces of specimens (HS170 M).

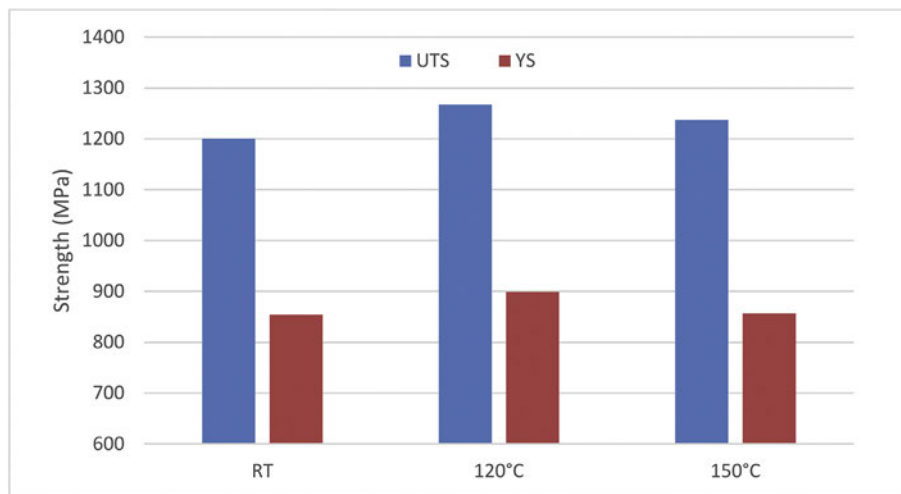


Fig. 3. Strength of HS170 M as a function of temperature.

threshold. For this reason, the discrimination threshold occasionally had to be manually adjusted in order to generate black and white images, which could be analyzed by the image analysis software.

Specimens of HS170 M submitted to different testing conditions, some reproducing the operating conditions of an engine, were studied. Four specimens were from tensile tests (TS) and three were from connecting rods (CR). Table 3 summarizes the heat treatments and mechanical testing performed on these specimens.

3. Results of microstructural characterization

The spatial distribution of Cu was mapped by EDS in the SEM for the five materials shown in Table 1. Based on the Cu maps, the micro-hardness of ferrite was measured in areas with Cu as well as in areas without Cu, Fig. 6.

The presence of Cu hardens the steel for all of the materials tested. The increase of micro-hardness can be as high as 30% (Fig. 7). For comparison, the micro-hardness of pure ferrite, measured on pure Fe, is about 150 HV and that of pearlite, measured on 1080 steel, is about 300

HV.

Furthermore, SEM observations performed in the micro-hardness indentations show that the smaller indents (harder areas) contain very small precipitates (Fig. 8). An EDS analysis of the small precipitates confirms that they are Cu-based (Fig. 9).

In addition, extraction carbon replicas were employed to isolate the second phase precipitates and confirm their chemical composition. This technique has the advantage of dissolving the matrix surrounding the precipitates, which can then be analyzed with the help of transmission electron microscopy (TEM) without any interference from the base material holding them. It was shown that the second phase nano particles contain mainly copper [9].

A large number of detailed SEM observations showed that Cu precipitates were present in the areas containing Cu for all of the specimens described in Table 3. The volume fraction of Cu precipitates of specimens submitted to different heat treatments and mechanical testing was determined by image analysis (Table 4) performed on images similar to those shown in Fig. 10.

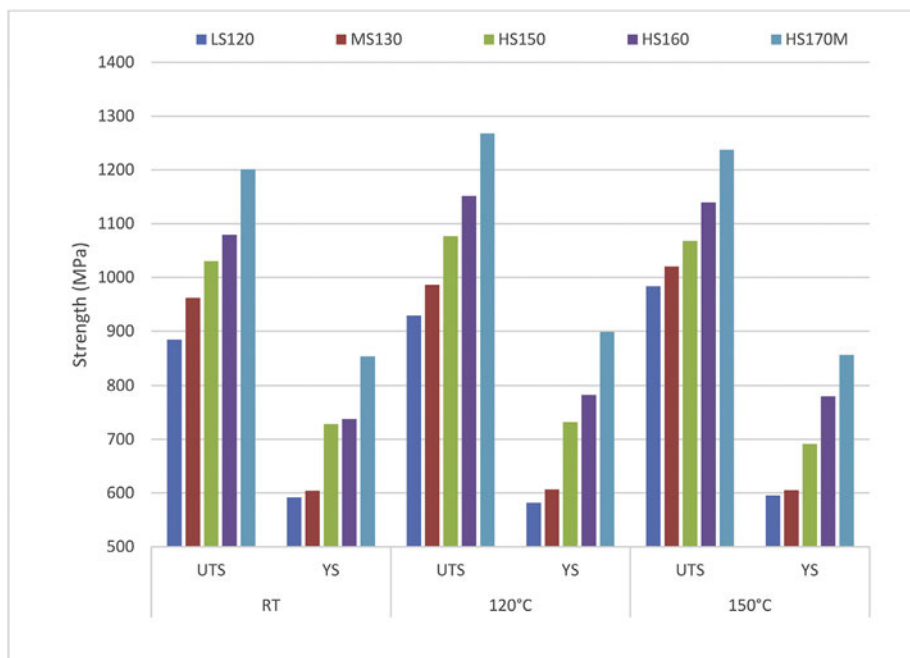


Fig. 4. Tensile strength of HS materials as a function of temperature.

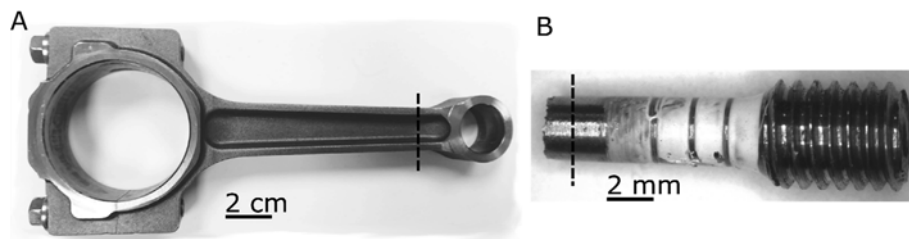


Fig. 5. Sections submitted to SEM investigations. A) For connecting rods. B) For tensile specimens.

Table 3

Heat treatments and mechanical testing of the specimens used for volume fraction measurements.

Specimen	Type of specimen	Conditions
TS RT	Tensile specimen	Tested at room temperature until rupture
TS 120	Tensile specimen	Tested at 120 °C until rupture
TS 120 Head	Tensile specimen	Threaded portion of the tensile specimen tested at 120 °C until rupture
TS 120i	Tensile specimen	Tested at 120 °C up to a stress level of 250 MPa (corresponding to a typical engine load) and then interrupted
CR F&Q	Connecting rod	Forged and air quenched
CR Aged	Connecting rod	Aged at 150 °C for 750 hours
CR Dyno	Connecting rod	Dyno tested at ~100 °C–150 °C for 750 hours (stress ranging from ~ −550 MPa to +350 MPa)

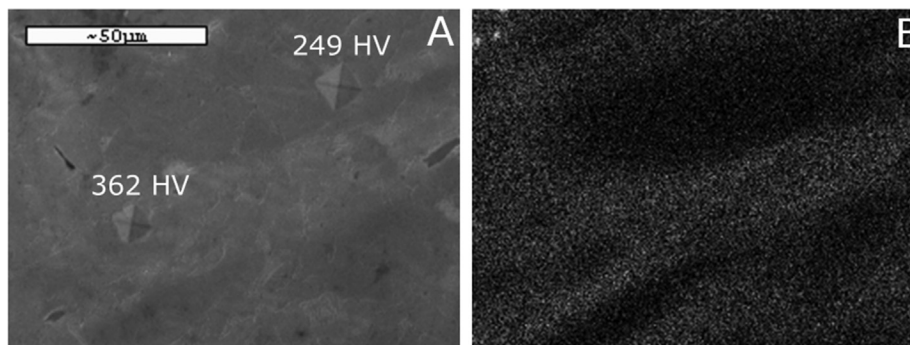


Fig. 6. A) SEM micrograph showing micro-hardness indentations and B) copper X-ray map of the same area. Micro-hardness measurements taken in areas with and without Cu (specimen HS170M, forged and air quenched).

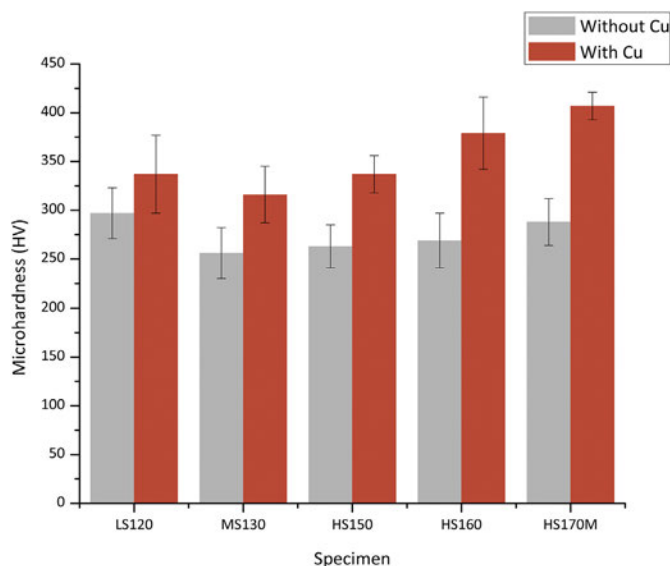


Fig. 7. Micro-hardness of ferrite with and without Cu for the five different materials shown in Table 1. Measurements taken on as-forged connecting rods.

4. Discussion

The forged and quenched connecting rod (CR F&Q) can be

considered as the as-received material from which all the other specimens listed in Table 4 are derived. It has the lowest volume fraction of Cu precipitates (0.19%). The tensile specimen tested at room temperature (TS RT) has a volume fraction of Cu precipitates similar to that of the CR F&Q (0.21% vs. 0.19% respectively), which shows that an applied stress at room temperature does not induce the precipitation of Cu. However, performing the tensile test at 120 °C more than doubles the volume fraction of Cu precipitates (0.46% vs. 0.21%). This is a clear indication that an applied stress at a relatively low temperature, such as 120 °C, even for a very short period, such as the duration of a tensile test, is promoting the precipitation of Cu. The threaded portion of the tensile specimen (TS120 Head) was also analyzed to determine the effect of the thermal cycle alone, without the effect of stress. The volume fraction of Cu precipitates in the threaded portion of the specimen is only slightly larger than that of the CR F&Q (0.25% vs. 0.19%), indicating that a temperature of 120 °C alone is not sufficient to cause the precipitation of a substantial amount of Cu. The specimen TS 120i was submitted to tensile testing at 120 °C, but the test was interrupted at a stress level of about 250 MPa, well below the YS of the material at RT (854.1 MPa, Table 2), in order to investigate the effect of elastic stresses. In this case, the volume fraction of Cu precipitates is larger than that of the CR F&Q (0.37% vs. 0.21%) but somewhat lower than that of the TS 120 specimen tested to failure (0.37% vs. 0.46%).

The specimen CR Aged is a connecting rod that was aged at 150 °C for 750 hours. The volume fraction of Cu precipitates is larger than that of the forged and quenched connecting rod (0.36% vs. 0.19%) and this difference can only be attributed to higher temperature and longer

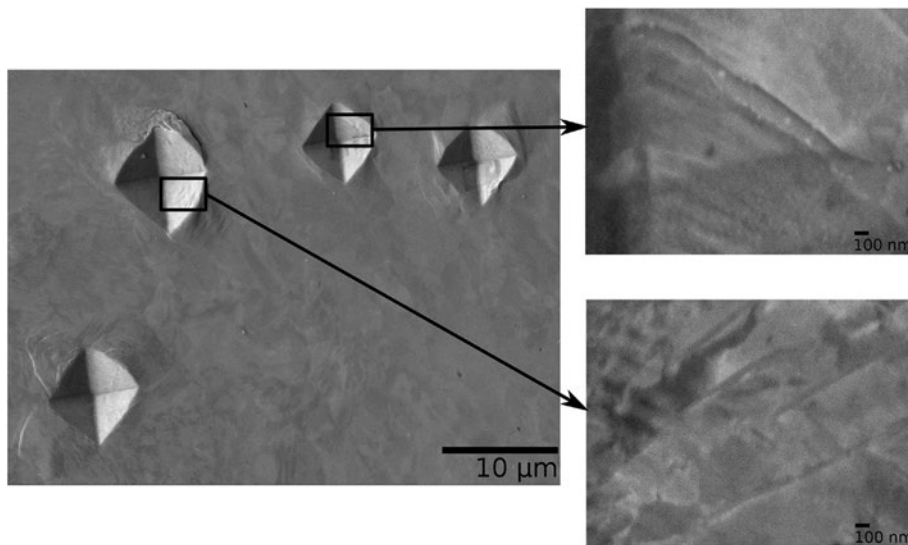


Fig. 8. Secondary electrons SEM micrograph (left) showing micro-hardness indentations. Backscattered electrons SEM micrographs (right) acquired in the indentations of areas with Cu (top right) and without Cu (bottom right). Copper precipitates can be seen in the smaller indentation (specimen HS170 M forged and air quenched).

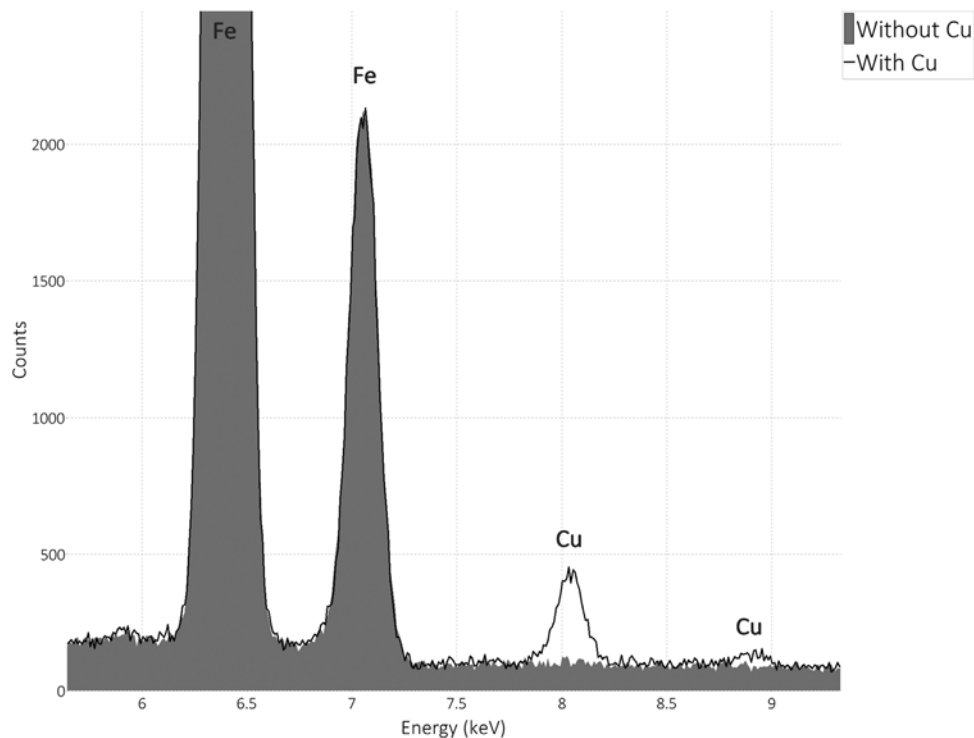


Fig. 9. X-ray EDS spectra showing the presence of Cu in the harder area (362 HV) and the absence of Cu in the softer area (249 HV). Specimen HS170 M forged and air quenched.

Table 4

Results of volume fraction measurements.

	TS RT	TS 120	TS 120 Head	TS 120i	CR F&Q	CR Aged	CR Dyno
Volume fraction (%)	0.21 ± 0.02	0.46 ± 0.04	0.25 ± 0.03	0.37 ± 0.03	0.19 ± 0.02	0.36 ± 0.03	1.02 ± 0.07
Average size (nm)	25 ± 3	22 ± 2	28 ± 3	27 ± 3	29 ± 3	28 ± 2	29 ± 2

time. However, if both heat and stress are applied concomitantly for longer periods of time, the precipitation of Cu can be greatly enhanced, as shown by the CR Dyno specimen, which is a connecting rod that was submitted to dyno testing for 750 hours at a temperature ranging between 100 °C and 150 °C (with a fluctuating elastic stress ranging from a low of about −550 MPa to a high of about +350 MPa). The volume fraction of Cu precipitates measured for the CR Dyno specimen is the

largest measured (1.02%). All of the results described so far confirm the combined effects of heat and stress resulting in larger amounts of Cu precipitation.

Since deformation induced by the applied stress appears to be a key factor of the precipitation process, thin lamellae of some of the materials listed in Table 3 were prepared. Bright and dark field TEM observations were carried out and several Cu precipitates, like the ones

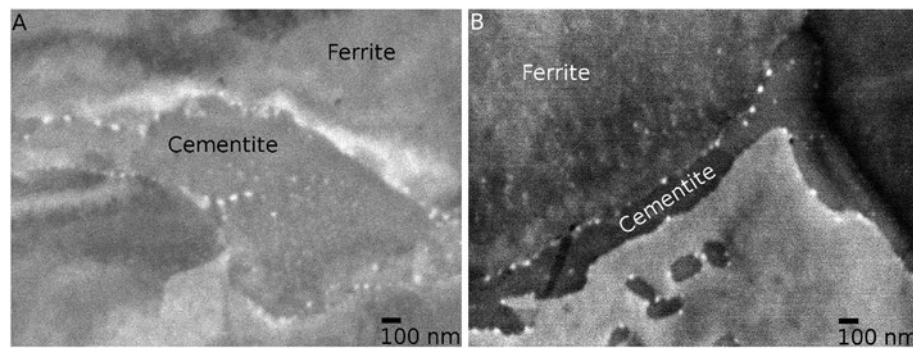


Fig. 10. A) Copper-rich precipitates in cementite and B) in cementite and ferrite (specimen CR Dyno).

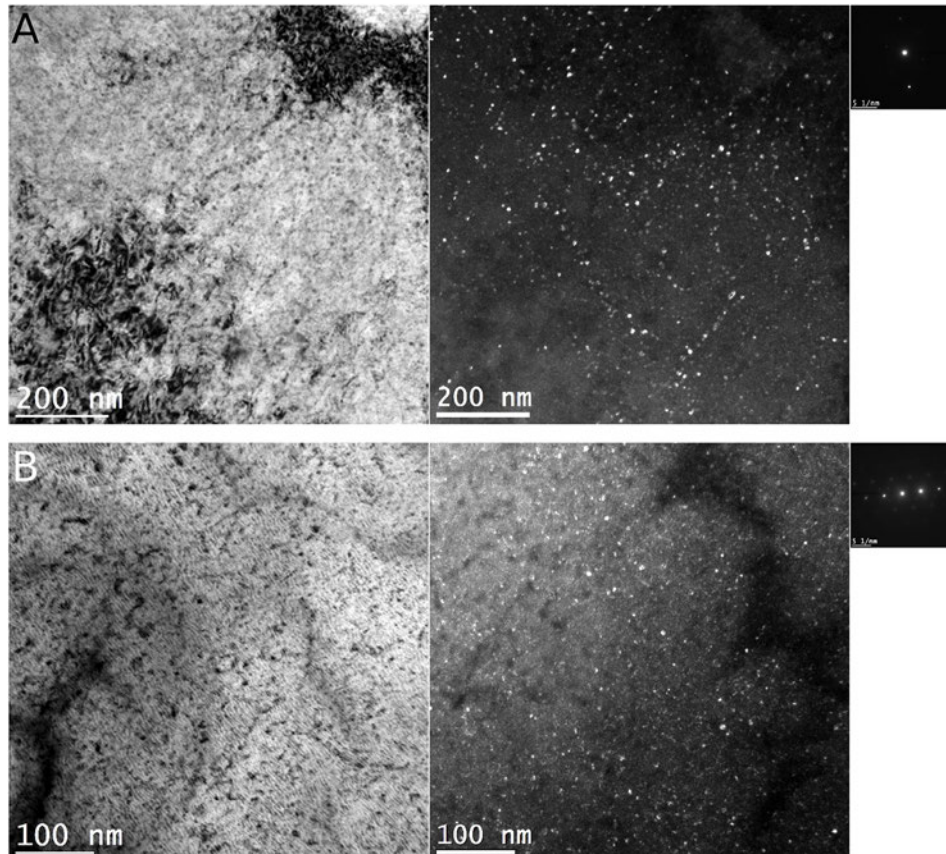


Fig. 11. Bright (left) and dark (right) field TEM micrographs showing Cu precipitates in A) TS 120, near B = [001] with $g = (200)$ and B) CR Dyno, near B = [111] with $g = (110)$.

shown in Fig. 11, were observed. Bright field images were acquired using the transmitted beam and therefore have a bright background while the dark field images were acquired using the diffracted beam, so that the background appears dark.

High spatial resolution EDS analyses (Fig. 12) show these small precipitates to be Cu rich. In addition, extraction replicas prepared to isolate the second phase precipitates from the surrounding matrix confirmed that they consist of Cu [9].

The solubility of Cu in Fe is negligible at room temperature or even at 120 °C or 150 °C [15]. Nevertheless, considering the inhomogeneity of elemental distribution due to the powder manufacturing process, the Cu content of the steel parts manufactured with HS170 M was measured by EDS in SEM, and copper-rich areas with up to 4.7 wt% Cu were found. Local supersaturation is therefore relatively large and contributes to an increase of the transformation energy and, as a result, a decrease in the critical nucleation energy for precipitation. At the early

stages, the supersaturation may be the most important factor contributing to the precipitation of Cu in ferrite. Once the precipitates reach a certain size, supersaturation ceases to be the dominant force for precipitation.

When stress is applied in operation or during mechanical testing at higher temperatures, as it is the case with the specimens studied in this work, the amount of dislocations increases and they will interact with the precipitates. TEM investigations showed that the precipitates decorate and pin the dislocations, as illustrated in Figs. 13–15.

Pinning of the dislocations will lead to an increase of the strength of these materials. The dislocations will in turn promote diffusion and act as nucleation sites for precipitates, thereby increasing their volume fraction. As the volume fraction of precipitates increases, so does their interaction with dislocations, making them less mobile and contributing to a further increase in strength. This dynamic interaction process between dislocations and precipitates leads to an increase of the

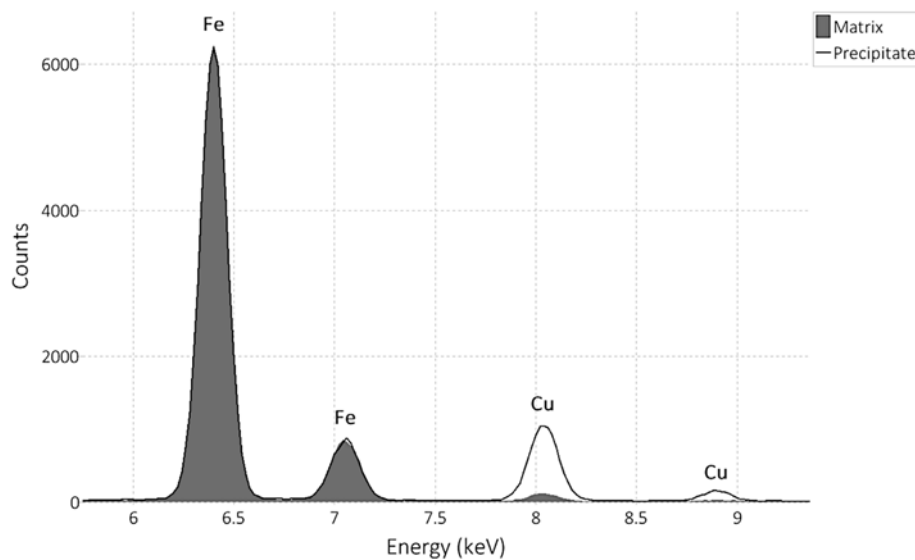


Fig. 12. EDS analyses showing the presence of Cu in the small precipitates in Fig. 10B). Specimen CR Dyno.

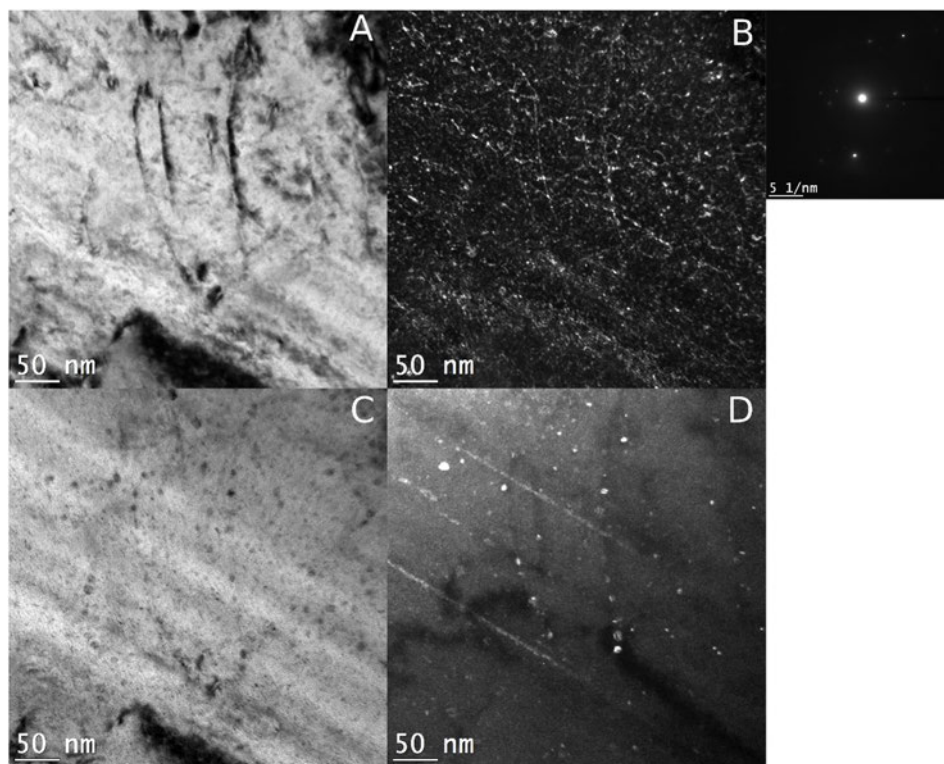


Fig. 13. TEM micrographs showing dislocations decorated by Cu-rich precipitates (specimen CR Dyno). A) Bright field. B) Weak beam. C) Bright field with $S_g \gg 0$. D) Dark field. Near $B = [113]$ with $g = (211)$.

mechanical properties of these alloys in operation.

Although the component does not experience plastic deformation in operation, as reported in the literature, the precipitation process can be significantly accelerated due to the effect of only elastic deformation [16]. This phenomenon was proven by the increase in the volume fraction of precipitates in the case of specimens TS 120i and CR Dyno (Table 4), both of which were submitted to applied stress levels well below the yield strength of the material.

5. Conclusions

The yield and ultimate tensile strengths of Fe–Cu–C PM mixes used

to manufacture powder-forged connecting rods are higher at 120 °C and 150 °C than at room temperature.

The improved mechanical properties are the result of the precipitation of Cu and the dynamic interaction between dislocations and precipitates at temperatures as low as 120 °C. Time, heat, and applied stress, both elastic and plastic, contribute to increasing the volume fraction of the Cu precipitates. Precipitation is more pronounced in Cu-rich areas typical of PM materials.

The stresses applied during testing or from engine operating loads promote precipitation in the matrix and on dislocations. These precipitates in turn pin dislocations leading to increased strength.

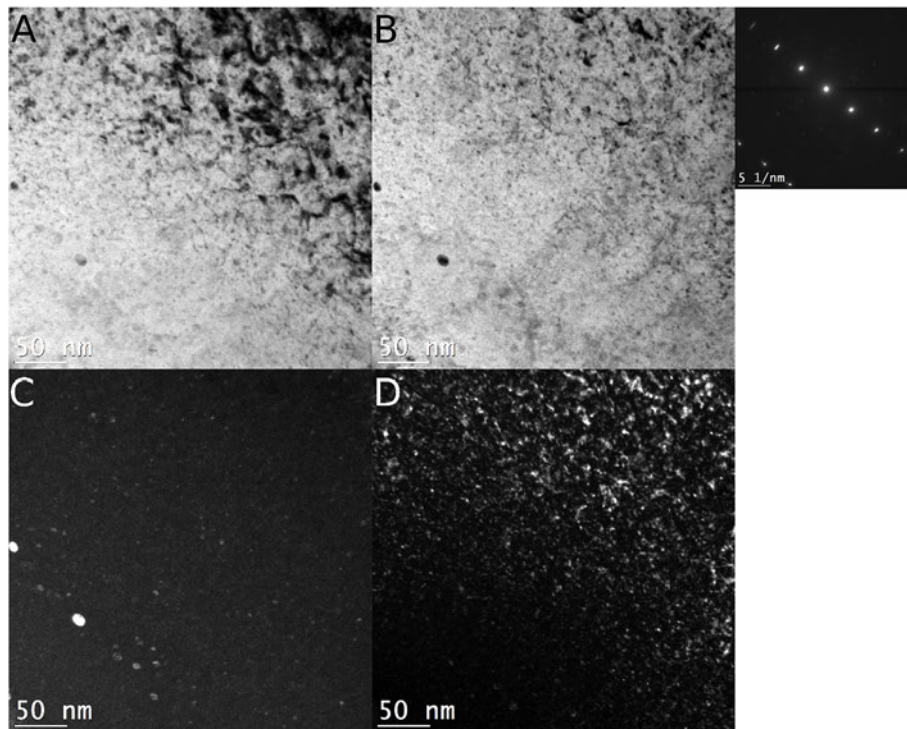


Fig. 14. TEM micrographs showing dislocations decorated by Cu-rich precipitates (specimen TS 120). A) Bright field. B) Bright field with $S_g \gg 0$ C) Dark field. D) Weak beam. Near $B = [133]$ with $g = (022)$.

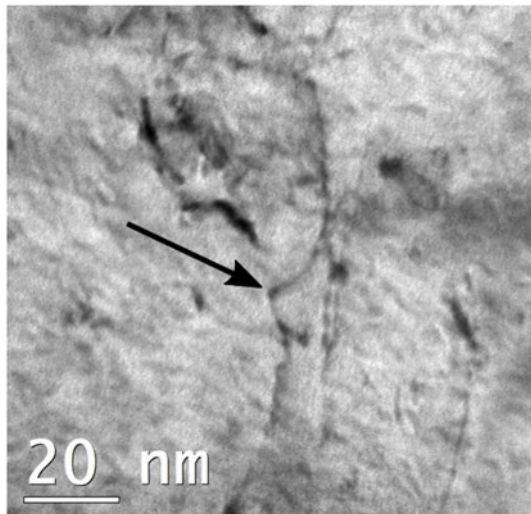


Fig. 15. Bright field TEM micrograph showing a dislocation pinned by a Cu-rich precipitate. Specimen CR Dyno.

Acknowledgement

The authors would like to acknowledge AAM (American Axle and Manufacturing) as well as CRITM (Consortium de Recherche et d'Innovation en Transformation Métallique) for funding.

References

- [1] ASM Handbook, ASM International, Materials Park, 1, 2005, p. 699.
- [2] S. Wang, et al., Effects of copper content on microstructure and mechanical properties of powder-forged rod Fe-Cu alloys manufactured at elevated temperature, *Mater. Sci. Eng. A* 743 (2019) 197–206.
- [3] K. Nakashima, et al., Interaction between dislocation and copper particles in Fe-Cu alloys, *ISIJ Int.* 42 (No. 12) (2002) 1541–1545.
- [4] D. Kapoor, The effect of heat treatment on sintered Fe-Cu alloys, *Heat. Treat.* (1978) 20–25.
- [5] F. Bernier, M. Gauthier, P. Plamondon, G. L'Espérance, Copper Strengthening of PM Steel Parts. *Advances in Powder Metallurgy and Particulate Materials*, San Francisco, (2011), pp. 9-142–9-153.
- [6] E. Ilia, K. Tutton, M. O'Neill, G. Lanni, Optimizing the Chemical Composition of the Materials Used to Manufacture Powder Forged Connecting Rods. *Advances in Powder Metallurgy and Particulate Materials*, Denver, (2007), pp. 10-18–10-25.
- [7] E. Ilia, K. Tutton, G. Lanni, Overview of properties of the materials used to manufacture connecting rods. *World PM Congress*, Yokohama, (2012).
- [8] E. Ilia, The effect of copper precipitation on mechanical properties at operating temperature of the materials used to manufacture powder forged connecting rods, *Int. J. Powder Metall.* (2014) 11–20.
- [9] E. Ilia, et al., High Performance Powder-Forged Connecting Rods for Direct Injection Turbocharged Engines. *JSAE 20159850/SAE 2015-32-0850*, (2015).
- [10] R. Stone, *Introduction to Internal Combustion Engines*, third ed., Society of Automotive Engineers, 1999, p. 453.
- [11] D. Wang, O. Mian, D. Merritt, M. Praca, G. Zhu, Elasto-Hydrodynamic Lubrication Analysis and Wear Prediction for a Connecting Rod Small-End Bush and Piston Pin Interface, *Society of Automotive Engineers*, Detroit, 2008, p. 4. Technical Paper 2008-36-0068.
- [12] A. Ancas, D. Gorbanescu, Theoretical models in the study of temperature effect on steel mechanical properties. *Buletinul institutului politehnic din Iasi, tomul V11 (VIV), Fascism 1–2* (2006) 49–54.
- [13] I. Chen, B. Young, B. Uy, Behavior of high strength structural steel at elevated temperatures, *J. Struct. Eng.* 132 (12) (2006) 1948–1954.
- [14] Annual Book of ASTM Standards. Vol. 03.01, ASTM International, West Conshohocken, PA (2016), pp. 69 - 98 and 178 - 185.
- [15] Hiroaki Okamoto, Mark E. Schlesinger, Erik M. Mueller (Eds.), *ASM Handbook, Vol. 3: Alloy Phase Diagrams*, ASM International, 2016, pp. 2–168.
- [16] G. Sauthoff, Influence of Stresses on Precipitation, *J. Phys. IV* 111 (6) (January 1996) 87–97 Colloque C1, supplément au Journal de Physique.